

Introduction

Sleipner is the first commercial-scale CO₂ injection operation worldwide, injecting approximately one million metric tons per year (1 Mt/y) into the Utsira sand continuously since 1996. The Sleipner project has been immensely successful and builds confidence in the ability to handle large volumes of CO₂ from the point of capture to injection [7].

During the course of injection of nearly 16 million tons of CO₂ into the Utsira, the plume has been under continuous observation through application of several geophysical monitoring techniques. This includes 6 repeat seismic surveys performed in the years 2001, 2002, 2004, 2006 and 2008. These unique datasets are valuable for understanding the important physical processes affecting movement of CO₂ in the subsurface [1]. Additionally, the data can be used to verify and validate modeling tools and commercial simulators. By matching to data, models can be properly calibrated and subsequently used to predict CO₂ movement in future years.

An important aspect of understanding CO₂ migration in large-scale projects is the benchmarking of models. There are many available simulators available that can handle multiphase and multiphysics fluid flow of CO₂ in brine aquifers. These models differ to a varying degree in the processes that are modeled and the solution method. Due to the inherent complexity of multiphase flow in porous media, all models must make a certain number of assumptions to simplify the system. Therefore, different models should be benchmarked to understand how variations in model complexity affect the predicted solution. Ideally, benchmarks should be performed against available data, such as the Sleipner seismic data. To this end, the seismic data from the topmost unit in the Utsira sand, Layer 9, have been released along with other parameters of the system [16].

The Layer 9 seismic data show that the system is gravity-dominated while the direction and speed of CO₂ migration is controlled by the topography of the top of the Utsira Formation [16]. CO₂ has formed a relatively thin layer underneath the shale caprock, collecting in local structures. As the system evolves, CO₂ accumulates in these small features until reaching a spill point and flowing upslope into the next structure. By 2002, it became evident that CO₂ was flowing away from the injection point preferentially along a north-trending ridge.

To date, no existing model or commercial simulator has been able to reproduce the details of the Layer 9 dataset. This may be due to a poor understanding of the physical parameters affecting flow or to insufficient modeling capabilities, or both. Standard full-physics 3D models such as Tough2, Eclipse 100 or 300 [15] lead to excessively dispersive results around the point of injection [1], which could be due to poor resolution of the vertical location of the CO₂-brine interface. Another technique based on invasion-percolation is able correctly capture the upslope migration of CO₂ along the ridge, but does not allow for viscous effects close the point of injection and thus underestimates lateral and downslope CO₂ migration [16].

We propose an alternative modeling approach, the VE model, which is based on the vertical equilibrium assumption. The VE model assumes negligible vertical flow and complete gravity segregation as a basis for reducing the full three-dimensional system of equations to two lateral dimensions [13]. The resulting 2D equations are then solved by numerical methods for heterogeneous and structurally complex systems [5]. Given the gravity-dominated nature of CO₂ in the Utsira Formation seen in the seismic data, the VE model can be appropriately applied to this system. We use the seismic data to constrain parameter uncertainty given a gravity-dominated system. We focus on CO₂ density, porosity, and topography of the top Utsira. The principle objectives of this study are: (1) to demonstrate the VE model can effectively capture the dominant flow physics occurring in the Utsira Formation; (2) to understand how uncertainty in important input parameters affects CO₂ migration; and (3) what range of uncertainty in CO₂ and rock properties is supported by the data.

Method

The VE model formulation is based upon vertical integration of the three-dimensional flow equations under the assumption that the fluids are in vertical equilibrium and the fluids are completely segregated due to gravity [10]. These assumptions are reasonable for modeling CO₂ injection into the Utsira Formation because it is a gravity-dominated system. The fluids segregate within months to a year due to a high average permeability (1 Darcy), strong buoyancy forces (density contrast $\Delta\rho$ on the order of 300 to 600 kg/m³) and a large aspect ratio (5 kilometers in lateral extent compared with 20-100 meters in reservoir thickness) [17]. The VE model has been employed historically for strongly segregated flows in petroleum reservoirs [3, 2, 10, 9] and more recently for CO₂ sequestration in saline aquifers [12, 11, 8, 4, 13].

To derive the VE model, the 3D equations are integrated over an aquifer (or sublayer of the aquifer if the permeability is stratified) with top and bottom boundaries whose vertical locations are described by functions $\zeta_T(x, y)$ and $\zeta_B(x, y)$, respectively. Within this aquifer, two mobile fluid phases exist, CO₂ and brine, along with associated residual phases. The vertical location of the CO₂-brine interface at any point in lateral space is given by $\zeta_M(x, y, t)$. Dissolution of CO₂ into the brine phase or vice versa [4] or capillary effects [14] are not considered in this study. The full VE model has been derived elsewhere [4, 5, 13], and only a summary of the 2D equations is given herein.

Conservation of mass equation in 2D for components CO₂ and brine,

$$\frac{\partial}{\partial t} (H\Phi S_\alpha) + \nabla_{\parallel} \cdot \mathbf{F}_{\parallel\alpha} = Q_\alpha, \quad \alpha = c, b. \quad (1)$$

In the integrated equation, Φ is depth-averaged porosity, S_α is the depth-integrated saturation, $H(x, y)$ is spatially varying aquifer thickness, defined as $H(x, y) = \zeta_T(x, y) - \zeta_B(x, y)$, Q_α is the depth-integrated source/sink term, $(\cdot)_{\parallel}$ represent lateral operators and quantities. Capital letters indicate vertically up-scaled variables.

Depth-integrated saturation is defined as

$$H\Phi S_\alpha = \int_{\zeta_B}^{\zeta_T} \phi s_\alpha dz, \quad \alpha = c, b. \quad (2)$$

The mass fluxes $\mathbf{F}_{\parallel\alpha}$ are obtained by vertically integrating the lateral component of phase fluxes and gives the resulting upscaled flux expression,

$$\mathbf{F}_{\parallel\alpha} = \int_{\zeta_B}^{\zeta_T} \mathbf{u}_{\parallel\alpha} dz, \quad \alpha = c, b. \quad (3)$$

Assuming the lateral gradients in pressure are constant in the vertical dimension, the resulting depth-integrated flux expression is,

$$\mathbf{F}_{\parallel\alpha} = -\frac{H\mathbf{K}_{\parallel\alpha} \cdot \mathbf{K}_{\parallel}}{\mu_\alpha} \cdot (\nabla_{\parallel} p_\alpha - \rho_\alpha \mathbf{g}_{\parallel}), \quad \alpha = c, b. \quad (4)$$

where \mathbf{K}_{\parallel} is the depth-integrated permeability tensor given by

$$H\mathbf{K}_{\parallel} = \int_{\zeta_B}^{\zeta_T} \mathbf{k}_{\parallel} dz, \quad (5)$$

and $\mathbf{K}_{\parallel\alpha}$ is the depth-integrated relative permeability tensor of phase α given by,

$$H\mathbf{K}_{\parallel\alpha} \cdot \mathbf{K}_{\parallel} = \int_{\zeta_B}^{\zeta_T} \mathbf{k}_{\parallel} k_\alpha dz, \quad \alpha = c, b. \quad (6)$$

For convenience, we will omit the $(\cdot)_{||}$ notation from this point forward.

Since pressure is in vertical equilibrium based on the Dupuit approximation [10, 4, 13], the phase pressure p_α in Equation (4) can be determined from a reference phase pressure P_α calculated at some datum level, $z = \zeta_P$. For the expressions that follow $\zeta_P = \zeta_B$. The reference phase pressures can be related by the location of the ζ_M interface and local capillary pressure. Since we have neglected local capillary pressure, then $P_n - P_b = \mathbf{e}_3 \cdot \mathbf{g} \Delta \rho (\zeta_M - \zeta_B)$, where $\Delta \rho = \rho_b - \rho_c$. Using $P = P_b$ as the primary pressure variable we obtain the following local pressure distribution for each phase,

$$p_b = P + \mathbf{e}_3 \cdot \mathbf{g} \rho_b (z - \zeta_B), \text{ for } \zeta_B \leq z \leq \zeta_M, \quad (7)$$

and

$$p_c = P + \mathbf{e}_3 \cdot \mathbf{g} [\rho_b (\zeta_M - \zeta_B) + \rho_c (z - \zeta_M)], \text{ for } \zeta_M \leq z \leq \zeta_T. \quad (8)$$

We see that the pressure is not obtained for a phase where it is immobile. By substitution of Equations (7) and (8) into Equation (4) we have,

$$\mathbf{F}_b = -\frac{H\mathbf{K}_b \cdot \mathbf{K}}{\mu_b} \cdot [\nabla P - \nabla (\mathbf{e}_3 \cdot \mathbf{g} \rho_b \zeta_B) - \rho_b \mathbf{g}], \quad (9)$$

and

$$\mathbf{F}_c = -\frac{H\mathbf{K}_c \cdot \mathbf{K}}{\mu_c} \cdot [\nabla P + \nabla (\mathbf{e}_3 \cdot \mathbf{g} \Delta \rho \zeta_M) - \nabla (\mathbf{e}_3 \cdot \mathbf{g} \rho_b \zeta_B) - \rho_c \mathbf{g}]. \quad (10)$$

Note that the z terms in expression Equations (7) and (8) disappear when taking the lateral gradient of p_α .

Together, Equations (1)–(10) represent the fine-scale system of equations consisting of depth-integrated variables. The VE model, which can be solved analytically under certain simplifying assumptions, must be solved numerically for heterogeneous systems (see [6, 5]). The fine-scale VE model must also resolve the topographical heterogeneity of the caprock to correctly capture fluid flow in a rough caprock system.

Some further assumptions can be made that allow for simplification of the integral expressions in Equations (2)–(6) above. First, we assume vertically homogeneous porosity and permeability ($\Phi = \phi$ and $\mathbf{K} = \mathbf{k}$) over the aquifer thickness, but still allow for horizontal variability. Then, capillary effects are assumed to be small in the Utsira, and therefore the transition zone in saturation at the CO₂-brine interface is relatively small and a sharp interface can be assumed. Thus, local CO₂ saturation above the ζ_M is equal to the end-point saturation ($s_c^0 = 1 - s_{wr}$), and zero below the interface. By introducing the thickness of the CO₂ phase, $h_c(x, y, t) = \zeta_T - \zeta_M$, and brine, $h_b(x, y) = \zeta_M - \zeta_B$, and considering only drainage conditions, we obtain the following simplified expressions,

$$S_c = (1 - s_{wr}) \frac{h_c}{H}, \quad S_b = \frac{h_b}{H}, \quad (11)$$

$$K_c = k_{rc}^0 \frac{h_c}{H}, \quad K_b = \frac{h_b}{H}, \quad (12)$$

where k_{rc}^0 is the endpoint relative permeability of CO₂ with residual brine. We observe that the tensorial relative permeability functions reduce to scalars for vertically homogeneous media.

Examples

The VE model is applied to the Sleipner Layer 9 benchmark problem. The mean and uncertainty range of fluid and rock properties are provided in [16]. We have made further simplifications of the benchmark definition:

- permeability is homogeneous and isotropic;

- porosity is homogeneous;
- top and bottom shales are impermeable to flow;
- capillary pressure between the phases is zero;
- density and viscosity of CO₂ and brine are constant;
- drainage conditions only.

We performed a suite of simulations and compared the resulting CO₂ plume extent to the L9 seismic data at 4 time intervals. The examples include a base case, which uses the values assigned in the benchmark studies (or mean values when one was specified) plus a series of simulations that explore some of the uncertainty in the data. The relevant parameters for the base case are presented in Table 1.

Table 1 Relevant parameters used in all simulations, with the exception of those in bold that are varied in the sensitivity simulations.

Parameter	Symbol	Value	Unit
Brine density	ρ_b	1020	kg/m ³
Brine viscosity	μ_b	$6.9 \cdot 10^{-4}$	Pa·s
CO₂ density	ρ_c	700	kg/m ³
CO₂ viscosity	μ_c	$6 \cdot 10^{-5}$	Pa·s
Brine residual saturation	s_{br}	0.11	-
CO ₂ endpoint relative permeability	k_{rc}^0	0.75	-
Porosity	ϕ	0.36	-
Permeability (homogeneous & isotropic)	K	2	Darcy

The objective of this study was not to perform a rigorous history match, but instead to understand sensitivity to the chosen set of parameters. Due to the gravity-dominated nature of fluid flow and the proximity of temperature and pressure at the top of the Utsira Formation, we chose parameters that have a significant impact on fluid migration and spatial distribution and have a large range in uncertainty—porosity, topography, and CO₂ density and viscosity. Other parameters could be chosen that have significant uncertainty such as injection rate into Layer 9, the strength of convective mixing on CO₂ dissolution, or capillarity, but we will leave that to a future study.

The Utsira porosity has been measured to have a mean value of 36% and a range of 27-40%. We chose two porosity values of 36% and 27% to test in this study, which are the mean and minimum values, respectively.

We also varied the CO₂ density and viscosity because of the sensitivity to temperature and pressure near the critical point. At the top of the Utsira, which is around 800 m depth, CO₂ density may vary between 400 and 700 kg/m³ due to just a few degrees uncertainty in temperature. Viscosity may also vary between 0.025 and 0.05 cP under similar uncertainty.

Likewise, the caprock topography data ($\zeta_T(x, y)$) provided for the benchmark may have an error of ± 10 m in depth due to the uncertainty in interpretation of seismic data. We tested several permutations of the caprock surface. To do this, a mean surface $\tilde{\zeta}_T(x, y)$ was fitted to the depth data using the `fit` function in Matlab with the local quadratic regression option. Then, the following weighted permutation function was used to create a total of 6 different caprock surfaces $\hat{\zeta}_T(x, y)$,

$$\hat{\zeta}_T = \zeta_T + \alpha \varepsilon_T \frac{\Delta \zeta_T}{\max(\Delta \zeta_T)} \quad (13)$$

where $\Delta\zeta_T = \zeta_T - \bar{\zeta}_T$, the error $\varepsilon_T = 5$ m, and the parameter $\alpha \in (-1, 1)$. The above equation gives two new surfaces having the maximum and minimum permutations from the original surface data. An additional 4 surfaces were generated by applying the permutation function only at local maxima (traps) where $\Delta\zeta > 0$ or only at local minima (spillpoints) where $\Delta\zeta < 0$. Finally, simulations were carried out using the mean fitted surface $\bar{\zeta}_T$ as the top surface of the domain.

Details of the parameters for the sensitivity simulations are given in Table 2 and 3.

Table 2 *Sensitivity study parameter values for rock and fluid properties.*

Parameter	Base Case	“Low” Cases
Porosity (%)	36	27
CO ₂ density (kg/m ³)	700	400
CO ₂ viscosity (Pa-s)	$6 \cdot 10^{-5}$	$1.65 \cdot 10^{-5}$

Table 3 *Parameters for permutation of Top Utsira topography.*

Case	α	Conditions on $\Delta\zeta_T$
Base	0	–
maxUpDn	1	for all $\Delta\zeta_T$
minUpDn	-1	for all $\Delta\zeta_T$
maxUp	1	$\Delta\zeta_T > 0$
minUp	-1	$\Delta\zeta_T > 0$
maxDn	1	$\Delta\zeta_T < 0$
minDn	-1	$\Delta\zeta_T < 0$

Results

The first simulation results for the the base case (Figure 1) show that CO₂ collects around the injection point and is contained within a local topographical maximum. Over time, the CO₂ spreads laterally in all directions and begins to move northward along the ridge by 2008. The plume is asymmetric and conforms to the topographical structure. At each reported time, the simulation results are contained within the bounds of the seismic data and matches well to the plume shape in the area near the injection point. However, the plume outline from seismic shows an early northward migration along the ridge from 2002, which is not captured by the base case simulation.

Sensitivity to Fluid/Rock Properties

We performed three sensitivity simulations: 1) low porosity only; 2) low CO₂ density/viscosity only; and 3) both low porosity and CO₂ density/viscosity. These tests were performed using the base case top Utsira topography, and the results are shown in Figure 2.

We observe that the effect of reduced porosity alone leads to more pronounced spreading of the plume compared to the base case. This results in a faster northward migration, however there is excess lateral migration to the west of the injection point. Despite the faster movement along the ridge, the reduced porosity only approaches but does not match the northern extent of the plume at any time.

Choosing low CO₂ density/viscosity values, but using the mean porosity, also results in faster migration along the ridge over time due to a higher density contrast and more unfavorable mobility ratio. In this case, CO₂ reaches the farthest northern extent of the plume as observed in the 2008 seismic data. The simulated plume retains a more compact shape and stays within the seismic data outline, but the match to the southward portion of the plume is poorer than the base case.

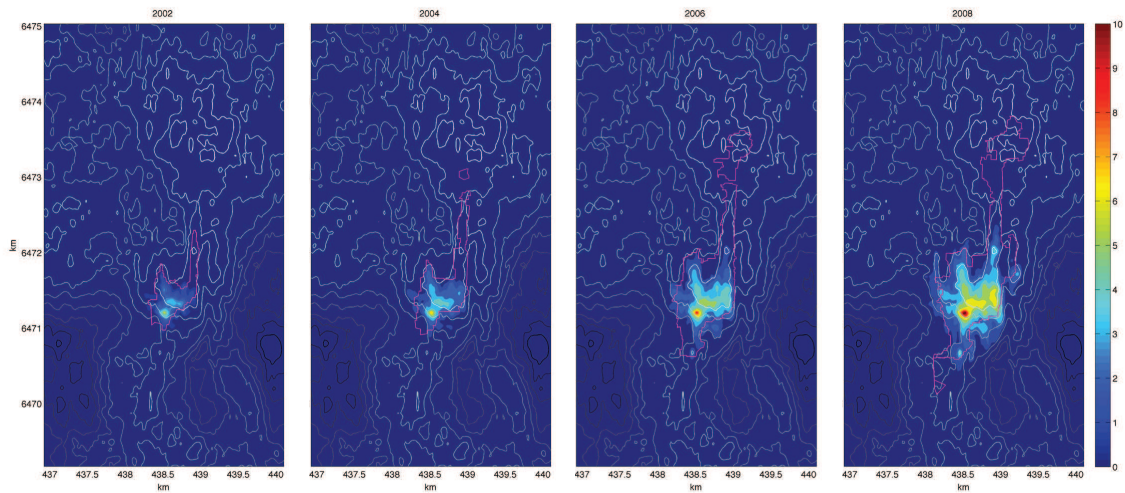


Figure 1 Simulation results of CO₂ injection into Layer 9 for the base case using parameter values provided by the benchmark definition. The CO₂ footprint observed in the seismic data is shown in magenta. Color scale indicates a CO₂ plume thickness between 0 and 10 meters.

Combining a reduced porosity with reduced CO₂ density and viscosity leads to the best match to the seismic data of these simulations. The match for 2002 and 2004 is nearly exact, with only a slight underestimation of southwestern extent of the plume. In 2006, the results predict less CO₂ at the north plume edge than observed in the seismic data. By 2008, the match to seismic improves in both the upslope and downslope directions.

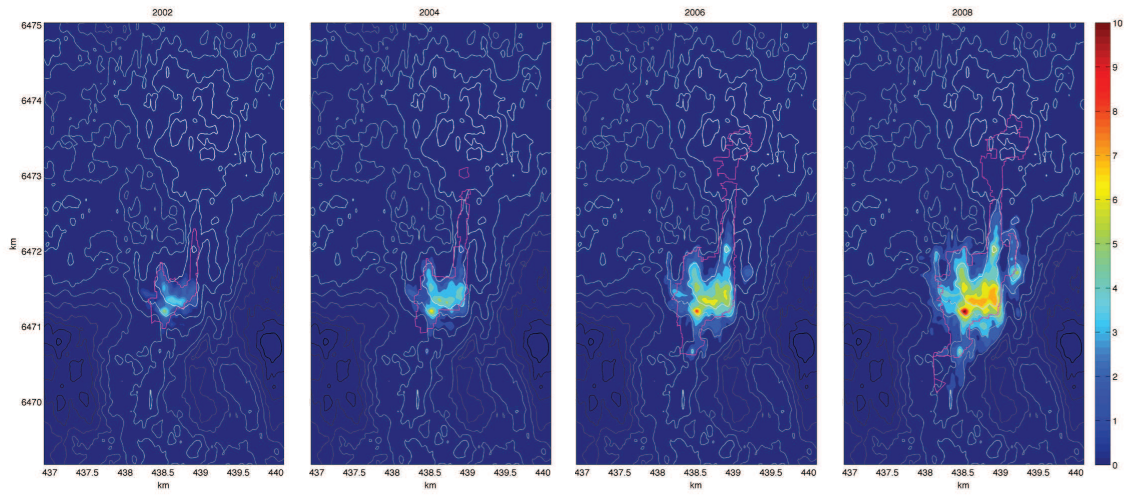
Uncertainty in Top Utsira Topography

Additional simulations were performed to understand the impact of uncertainty in the top Utsira data. Simulations were performed on each of the 7 modified surfaces described in Table 2 with the base case fluid and rock properties. In addition, 3 more simulations were performed on each surface using the low porosity and low CO₂ density/viscosity values to test the combination of uncertainty in rock and fluid properties and topography.

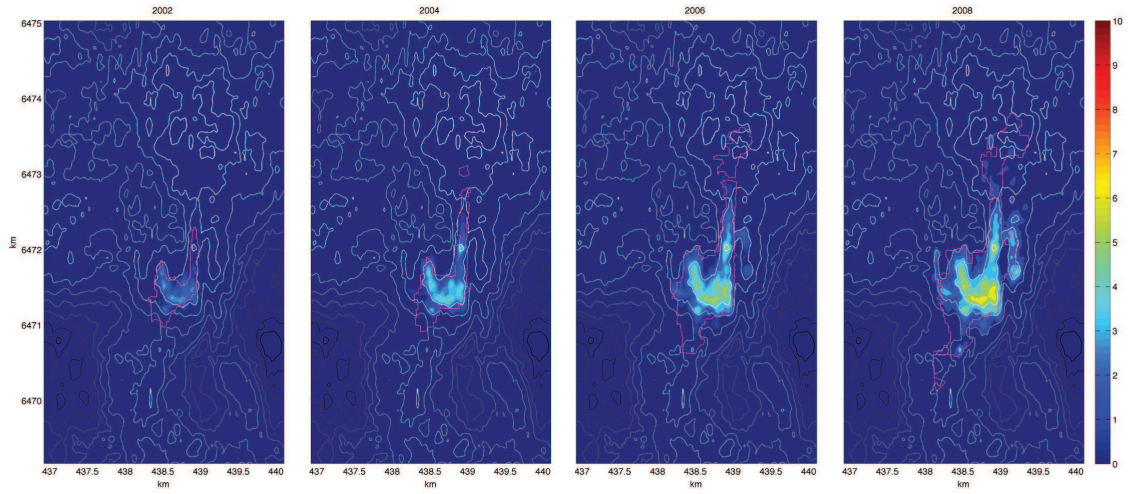
Due to the large number of simulations (28 in total), we discuss only the surfaces in which the local surface minima (spillpoints) were decreased in depth and/or the the local surface maxima (traps) were increased in depth. These correspond to “minXX” cases in Table 3. Only the 2008 simulation data will be compared to seismic data.

The results show that as the surface becomes smoother the plume shape becomes more symmetric around the injection point (Figure 3a). There is only a slight difference between the first three surfaces that minimize the spillpoints and traps. The solution is most sensitive to reducing the depth of the spillpoints than the traps (comparing (i) to (iii)). When the spillpoints are shallower, CO₂ can migrate more quickly from trap to trap, all else being equal. We see that CO₂ extends farther along the northward ridge in Fig. 3a(iii), but also, there is more lateral spreading as well. The sensitivity to spillpoints is reasonable given the gravity-dominated nature of the system.

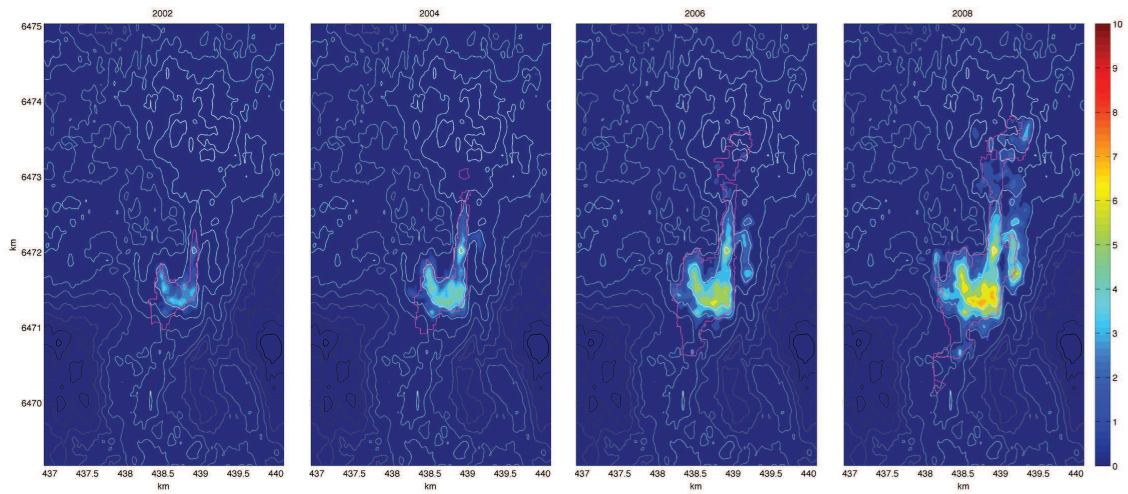
The mean fitted surface is the smoothest topography and has the greatest impact on CO₂ migration for lower porosity and CO₂ density (Figures 3c and 3c). By 2008, CO₂ has migrated much more quickly to the northeast than in any other cases. The plume is also spread over a greater area due to the lack of local traps and spillpoints to confine the plume near the injection point.



(a) Utsira porosity = 27%

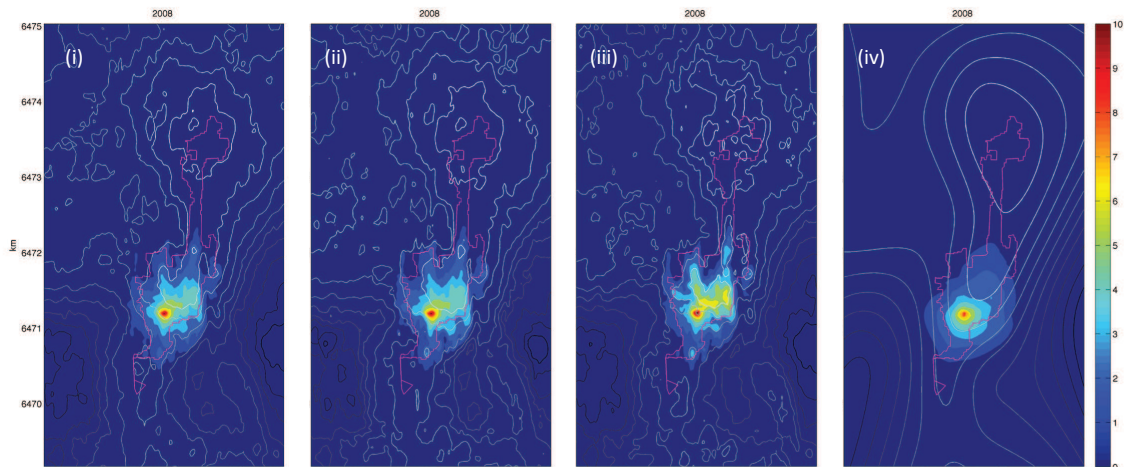


(b) CO₂ density = 400 kg/m³

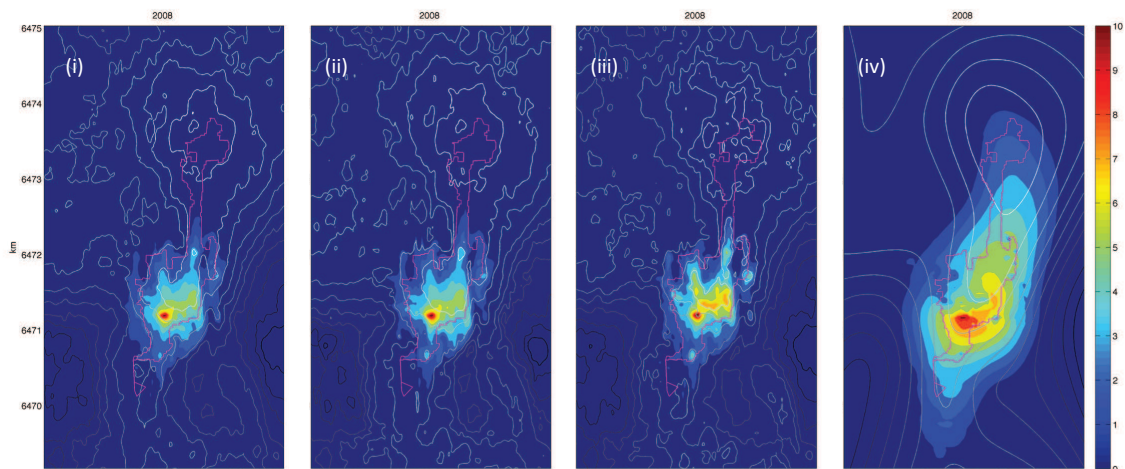


(c) Utsira porosity = 27%, CO₂ density = 400 kg/m³

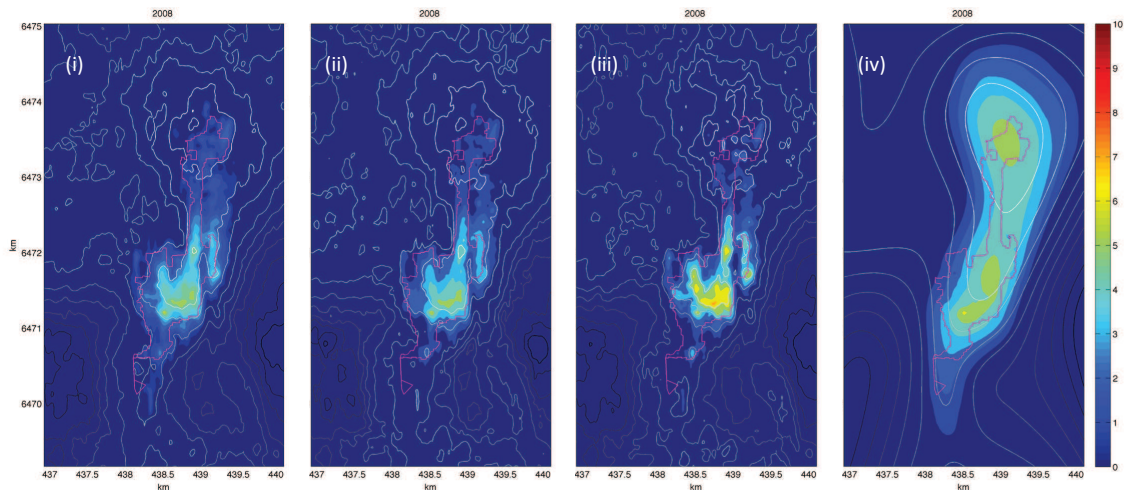
Figure 2 Simulation results of CO₂ injection into Layer 9 showing sensitivity to low values of Utsira porosity and CO₂ density and viscosity.



(a) Utsira porosity = 27%



(b) CO₂ density = 400 kg/m³



(c) Utsira porosity = 27%, CO₂ density = 400 kg/m³

Figure 3 Simulation results of CO₂ injection into Layer 9 showing sensitivity to topography variation: (i) minimized traps and spillpoints; (ii) minimized traps only; (iii) minimized spillpoints only; and (iv) mean fitted surface. Panels from top to bottom show sensitivity to low values of Utsira porosity and CO₂ density and viscosity for these surfaces.

Upslope Migration and Footprint

The farthest extent of the plume migrates away from the injection point approximately linearly in time for all cases with non-smooth topography (Figures 4a and 4b). The impact of rock and fluid properties leads to a large variation in migration speed, which results in a factor of 2 difference in upslope extent by 2008.

The change in spillpoint and trap depth has less impact on plume migration speed than rock and fluid properties (Figure 4b). For the low porosity case and baseline CO₂ properties, the difference in plume location is 10% by 2008. The difference is greater for the low CO₂ density/viscosity cases, with a 15% difference after 9 years of injection.

The smooth surface results (Figure 4c) in the largest difference in migration speed and extent. The farthest upslope extent is for the low porosity and low CO₂ properties, reaching nearly 4 km by 2008. In contrast, the baseline case for the smoothed surface reaches 1.5 km, which is only slightly farther than the base case simulation in Figure 4a.

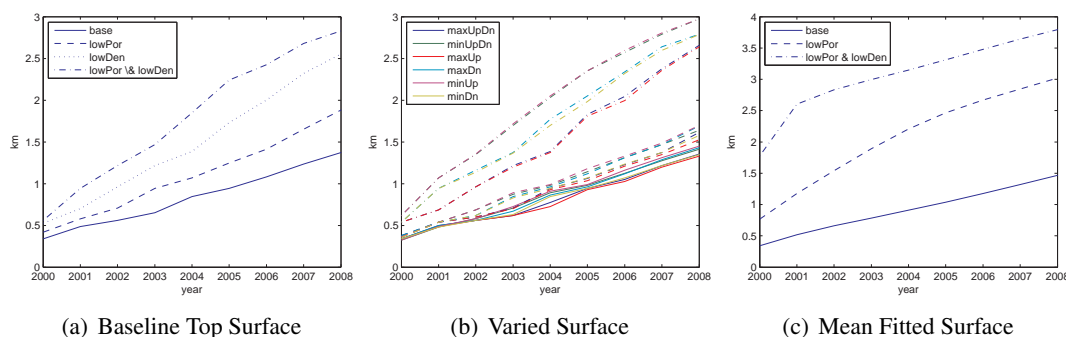


Figure 4 Maximum upslope extent from injection point.

The footprint area (measured in km²) of the plume is also affected by rock and fluid properties (Figure 5a). We observe a parabolic increase in areal extent over time with a larger area obtained with lower porosity and lower fluid properties. The difference between these cases is a factor of 1.5, which is less pronounced than for upslope extent measure discussed above.

The impact of topography variation leads to a similar magnitude of difference in areal extent as rock and fluid properties. Thus, across all cases in Figure 5b, the areal extent varies by more than factor of 2 between 1.5 and 3.25 km².

The mean fitted surface shows that without spillpoints and local traps, the maximum areal extent increases by a factor of 2 for the baseline rock and fluid properties, and by nearly 4 times for the lowest rock and fluid properties tested here.

Conclusions

From this study we can make the following conclusions:

- VE models are suitable for simulating CO₂ injection into gravity- and topography-dominated systems, such as the Utsira formation.
- Benchmark simulation of injection into Layer 9 using prescribed parameter values show reasonable match to seismic data near the injection well. However, the results give a poor match to the northward upslope migration.
- Decreasing porosity to 27% and CO₂ density to 400 kg/m³, the lowest in the possible range of

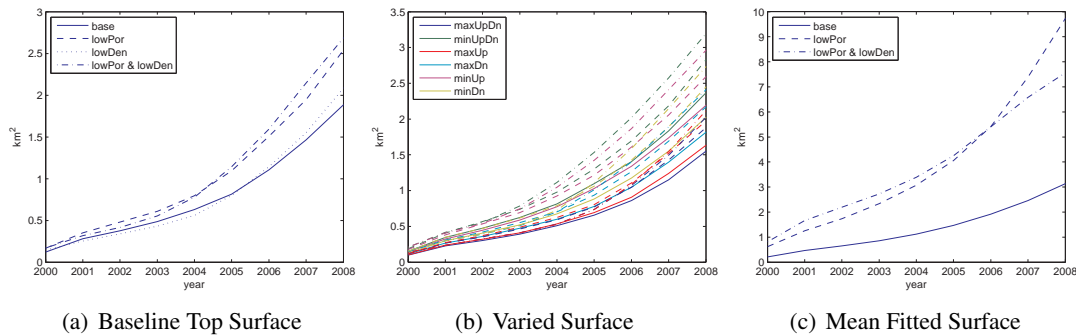


Figure 5 Areal footprint size.

values, speeds the upslope migration along the ridge as observed in the seismic data. The match to seismic is better as porosity and density decreases. The upslope migration is most sensitive to CO₂ density and viscosity, while reducing porosity gives a better match to the downslope migration. The case with lowest values for the sensitivity parameters gives the best overall match to seismic observations.

- Uncertainty in the top Utsira topography affects the match to seismic data. The depth of the spillpoints have the most impact on upslope migration, with shallower spillpoints leading to faster migration and greater spreading of the plume.
- The footprint of the plume is most affected by the presence of local traps that reduce spreading and contain the plume locally near the injection point. The baseline simulation results in a footprint of 1.5 km², while a perfectly smooth surface can reach up to 3 km² for the base case rock and fluid properties. With low porosity and CO₂ density, the plume can reach 10 km² in areal extent.
- The relative degree of uncertainty in individual parameters corresponds to the relative sensitivity of the solution to parameter variation. For instance, CO₂ density has a potentially large uncertainty compared to porosity and topography, and therefore the change in CO₂ properties has the greatest impact on the solution. However, if errors in topography estimation become large (> 5 m), then uncertainty in spillpoint depths will become as or more important overall.
- It is important to understand the impact of geological and fluid properties that control CO₂ migration in gravity-dominated systems. This will require numerous simulations to explore the large parameter space. Efficient modeling tools such as the VE model are well suited for this purpose.

Acknowledgements

This work was supported in part by the MatMoRA-II project (Mathematical Modelling and Risk Assessment of CO₂ storage), financed by the Research Council of Norway and Statoil. SEG is supported by the Statoil Akademia agreement with the University of Bergen.

References

- [1] Chadwick, R.A., Noy, D., Arts, R. and Eiken, O. [2009] Latest time-lapse seismic data from Sleipner yield new insights into CO₂ plume development. *Energy Procedia*, **1**, 2103–2110.
- [2] Coats, K., Dempsey, J. and Henderson, J. [1971] Use of vertical equilibrium in 2-dimensional simulation of 3-dimensional reservoir performance. *SPE J.*, **11**(1), 63–71.
- [3] Dietz, D.L. [1953] A theoretical approach to the problem of encroaching and by-passing edge water. *Proceedings of Akademie van Wetenschappen*, vol. 56-B, 83.
- [4] Gasda, S.E., Nordbotten, J.M. and Celia, M.A. [2011] Vertically-averaged approaches for CO₂ injection with solubility trapping. *Water Resources Research*, **47**, W05528.
- [5] Gasda, S.E., Nordbotten, J.M. and Celia, M.A. [2012] Application of simplified models to CO₂ migration and immobilization in large-scale geological systems. *International Journal of Greenhouse Gas Control*, in press.

- [6] Gray, W.G., Herrera, P., Gasda, S.E. and Dahle, H.K. [2011] Derivation of vertical equilibrium models for CO₂ migration from pore scale equations. *International Journal of Numerical Analysis and Modeling*, in press.
- [7] Hermanrud, C. et al. [2009] Storage of CO₂ in saline aquifers-lessons learned from 10 years of injection into the Utsira Formation in the Sleipner area. *Energy Procedia*, **1**(1), 1997–2004.
- [8] Hesse, M.A., Orr, F.M. and Tchelepi, H.A. [2008] Gravity currents with residual trapping. *Journal of Fluid Mechanics*, **611**, 35–60.
- [9] Huppert, H. and Woods, A. [1995] Gravity-driven flows in porous layers. *J. Fluid Mech.*, **292**, 55–69.
- [10] Lake, L. [1989] *Enhanced Oil Recovery*. Englewood Cliffs.
- [11] Neufeld, J.A. and Huppert, H.E. [2009] Modelling carbon dioxide sequestration in layered strata. *J. Fluid Mech.*, **625**, 353–370.
- [12] Nordbotten, J.M. and Celia, M.A. [2006] Similarity solutions for fluid injection into confined aquifers. *J. Fluid Mech.*, **561**, 307–327.
- [13] Nordbotten, J.M. and Celia, M.A. [2012] *Geological Storage of CO₂: Modeling Approaches for Large-Scale Simulation*. John Wiley & Sons, Inc.
- [14] Nordbotten, J.M. and Dahle, H.K. [2011] Impact of the capillary fringe in vertically integrated models for CO₂ storage. *Water Resources Research*, **47**, W02537.
- [15] Schlumberger Information Systems [2007] ECLIPSE technical description. Report, Houston, TX.
- [16] Singh, V., Cavanagh, A., Hanse, H., Nazarin, B., Iding, M. and Ringrose, P. [2010] Reservoir modeling of CO₂ plume behavior calibrated against monitoring data from Sleipner, Norway. *SPE 134891*, 2010 SPE Annual Technical Conference and Exhibition (ATCE), 19-22 September 2010 in Florence, Italy.
- [17] Yortsos, Y.C. [1995] A theoretical analysis of vertical flow equilibrium. *Transport in Porous Media*, **18**(2), 107–129, ISSN 0169-3913.